Optik

Sputtering power effects on the electrochromic properties of NiO films

--Manuscript Draft--

Manuscript Number:	
Article Type:	Full length article
Section/Category:	Optical Design
Keywords:	Thin film; Transition metal oxide; Electrochromic devices
Corresponding Author:	Juan Rubén Abenuz Acuña, M.D Universidad Autónoma de Ciudad Juárez Juarez, Chihuahua MEXICO
First Author:	Juan Rubén Abenuz Acuña, M.D
Order of Authors:	Juan Rubén Abenuz Acuña, M.D
	Israel Omar Pérez López, PhD
	Víctor Sosa Villanueva, PhD
	Fidel Fernando Gamboa Perera, PhD
	José Trinidad Elizalde Galindo, PhD
	José Rurik Farías Mancilla, PhD
	Diana María Carrillo Flores, PhD
	José Luis Enríquez Carrejo, PhD
	Luis Andrés Burrola Gándara, PhD
	Pierre Giovanni Mani González, PhD
Abstract:	The effect of sputtering power (P=60 W-180 W) on the electrochromic properties of nickel oxide films deposited on ITO-coated glass substrates by the radio frequency magnetron sputtering technique was investigated. Crystalline structure and morphology were assessed by X-ray diffraction and scanning electron microscopy, respectively. The effect of sputtering power on electrochromism of the samples was evaluated with cyclic voltammetry and chronoamperometry . A solution of LiClO4 in propylene carbonate was used for Li insertion/extraction. The chemical composition of the samples before and after Li intercalation were analyzed by X-ray photoelectron spectroscopy (XPS). We observed the cubic phase of NiO with sputtering power mainly affecting crystallinity and grain size. These in turn have an effect on the electrochromic properties. Coloration efficiency reduces from 8.03 cm^2 /A*s to 3.52 cm^2 /A*s as sputtering power increases from 60 W to 180 W. XPS analysis reveals that higher values of P promote the formation of nickel hydroxides on the film surface. As consequence of changes in crystallinity and morphology the presence of nickel hydroxides increases, showing that not only the electrochromic properties of the samples are affected by the sputtering power but also their chemical composition.
Suggested Reviewers:	Wang Hao Beijing University of Technology haowang@bjut.edu.cn Specialist in electrochromic properties of NiO.
	Aline Rougier Universite de Bordeaux Rougier@icmcb-bordeaux.cnrs.fr He have been participated in researches related to electrochromic properties of nickel oxide.
	Wenjie Mai Jinan University wenjiemai@gmail.com He have been participated in researches related to electrochromic properties of nickel

	oxide.
	Gamze Atak Hacettepe Teknokent AS gbaser@hacettepe.edu.tr Specialist in electrochromic properties of NiO.
	Rui-Tao Wen Uppsala University Ruitao.Wen@angstrom.uu.se Specialist in electrochromic properties of NiO.
Opposed Reviewers:	

Author Agreement Statement

In case that the present manuscript will be accepted, the Author agreement document will be presented. Thank you for understanding.

Impact Statement

Electrochromic materials as nickel oxide (NiO) are capable of changing their optical properties due ion intercalation as an electric field is applied. This material can be exploited to develop electrochromic devices with technology applications such as displays, touch screens, smart phones, sunglasses, smart windows, adjustable reflectivity car rear view mirrors, gas sensors and active optical filters among others. The electrochromic properties of nickel oxide films deposited by the radio frequency sputtering technique are affected by deposition parameters as annealing temperature, oxygen concentration, substrate temperature, etc. However, to our knowledge there are no works assessing the effect of sputtering power (*P*) on the electrochromic properties. This research focuses in study the effect of *P* on the electrochromic properties of NiO films deposited on ITO-coated glass. We investigate how the morphology, crystalline structure, the chemical ccomposition and electrochromic properties of the samples embedded in a $LiClO_4$ electrolyte are affected by sputtering power. Results indicate that morphology, crystalline structure, chemical composition and electrochromic properties can be modified trough sputtering power variations. We believe that these results can be contribute to the development of NiO-based electrochromic devices.

Juan Rubén Abenuz
Corresponding author
Department of Physics and Mathematics
Institute of Engineering and Technology
Autonomous University of Juarez City
Av. del Charro #450, Col. Romero Partido
C.P. 32310, Juárez, Chihuahua, México
E-mail : sanmaikel23@gmail.com

Cover Letter

June 8, 2020

Editor of Optik

Dear Sir or Madam

We would like to submit our manuscript entitled "Sputtering power effects on the electrochromic properties of NiO films", by Juan Rubén Abenuz Acuña *et. al.*, for possible publication in Optik. This work is original, has not either been published before or considered for publication elsewhere, and all co-authors agree with its contents.

This work focuses on reporting the effects of sputtering power on the electrochromic properties of nickel oxide (NiO) films deposited on ITO-coated glass by the radio frequency magnetron sputtering technique. We study the effects of sputtering power on morphology and crystalline structure, and, in turn, on the chemical and electrochromic properties of the samples embedded in a $LiClO_4$ electrolyte. Results obtained from this research invariably indicate that crystalline properties, morphology, chemical composition, and coloration efficiency of the samples can be altered trough sputtering power variations. We believe that these novel results can be useful in the development and design of NiO-based electrochromic devices.

It is because of these relevant findings and the current level of interest in NiO-based electrochromic devices that we feel our work is suitable for publication in Optik.

With kind regards
Juan Rubén Abenuz
Corresponding author
Department of Physics and Mathematics
Institute of Engineering and Technology
Autonomous University of Juarez City
Av. del Charro #450, Col. Romero Partido
C.P. 32310, Juárez, Chihuahua, México
E-mail : sanmaikel23@gmail.com
For your convenience, we would like to suggest some candidates for reviewers who you might consider for the evaluation of this manuscript.

Wang Hao- The College of Materials Science and Engineering, Beijing University of Technology, Beijing, 100124, PR China.
E-mail : haowang@bjut.edu.cn
Reason : Specialist in electrochromic properties of NiO.

Aline Rougier- CNRS, Univ. Bordeaux, ICMCB, UPR 9048, F-33600 Pessac, France.
E-mail: Rougier@icmcb-bordeaux.cnrs.fr
Reason : Specialist in electrochromic properties of NiO.

Wenjie Mai- Siyuan laboratory, Guangzhou Key Laboratory of Vacuum Coating Technologies and New Energy Materials, Department of Physics, Jinan University, Guangzhou, Guangdong 510632, China.
E-mail: wenjiemai@gmail.com
Reason : Specialist in electrochromic properties of NiO.

Sputtering power effects on the electrochromic properties of NiO films

Juan R. Abenuz Acuña[c,*], Israel Perez[a], Víctor Sosa[b], Fidel Gamboa[b], José T. Elizalde[c], Rurik Farias[c], Diana Carrillo[c], José L. Enríquez[c], Andrés Burrola[c], Pierre Mani[c]

[a] *National Council of Science and Technology (CONACYT)-Department of Physics and Mathematics, Institute of Engineering and Technology, Universidad Autónoma de Ciudad Juárez, Av. del Charro 450 Col. Romero Partido, C.P. 32310, Juárez, Chihuahua, México*
[b] *Applied Physics Department, CINVESTAV Unidad Mérida, km 6 Ant. Carretera a Progreso, A.P. 73, C.P. 97310 Mérida, Yucatán, México*
[c] *Department of Physics and Mathematics, Institute of Engineering and Technology, Universidad Autónoma de Ciudad Juárez, Av. del Charro 450 Col. Romero Partido, C.P. 32310, Juárez, Chihuahua, México*

Abstract

The effect of sputtering power (P=60 W-180 W) on the electrochromic properties of nickel oxide films deposited on ITO-coated glass substrates by the radio frequency magnetron sputtering technique was investigated. Crystalline structure and morphology were assessed by X-ray diffraction and scanning electron microscopy, respectively. The effect of sputtering power on electrochromism of the samples was evaluated with cyclic voltammetry and chronoamperometry. A solution of $LiClO_4$ in propylene carbonate was used for Li insertion/extraction. The chemical composition of the samples before and after Li intercalation were analyzed by X-ray photoelectron spectroscopy (XPS). We observed the cubic phase of NiO with sputtering power mainly affecting crystallinity and grain size. These in turn have an effect on the electrochromic properties. Coloration efficiency reduces from 8.03 cm^2/A·s to 3.52 cm^2/A·s as sputtering power increases from 60 W to 180 W. XPS analysis reveals that higher values of P promote the formation of nickel hydroxides on the film surface. As consequence of changes in crystallinity and morphology the presence of nickel hydroxides increases, showing that not only the electrochromic properties of the samples are affected by the sputtering power but also their chemical composition.

Key words: Thin film, Transition metal oxide, Electrochromic devices.

1. Introduction

Electrochromic materials are materials capable of changing their optical properties when ions are intercalated or deintercalated as an electric field is applied. Due to this peculiarity, these materials can be exploited to develop electrochromic devices (ECD), controlling in this way, properties such as transmittance and absorbance. Accordingly, some of the applications where these devices can be found are displays, touch screens, smart phones, sunglasses, smart windows, adjustable reflectivity car rear view mirrors, gas sensors and active optical filters among others [1–6]. An ECD is made of a pile of at least five layers of different materials in a sandwich arrangement. The external layers are transparent conductors where electric contacts are attached. Next, on each side, two electrodes are placed: one cathodic electrode and one anodic electrode; and in the middle an electrolyte is placed as ionic conductor. The applied voltage generates an electric field between the electrodes that makes ions flow from the electrolyte to an electrode. Ions eventually are displaced and captured in the crystalline lattice of one of the electrodes, modifying its optical properties [3, 4, 6, 7]. There are several inorganic compounds that are commonly used in the fabrication of electrodes for ECD. These are transition metal oxides (TMO) where TM is a transition metal such as W, Co, Ni, Ta, Mo, Ir, Ti, V, Mn, Nb, etc. The most studied oxide in ECD is WO_3 that has one of the largest coloration efficency among the oxides (54.8 cm^2/A·s at 633 nm) [10–13].

On the other hand, more recently, people have turned their attention to NiO [2, 3, 6–9]. Nickel oxide (NiO) is a semiconducting compound crystallizing in either cubic or hexagonal structure. The spatial group for the cubic phase is $Fm\bar{3}m$ with lattice parameter of 4.17 Å. This material exhibits properties of a p-type semiconductor with a band gap ranging from 3.4 eV to 4 eV [14–17]. Nickel oxide exhibits electrochromic properties that makes it a good candidate as an anodic material in ECD due to its low cost, good cyclic reversibility and its respectable coloration efficiency (CE=42 cm^2/A·s at 550 nm) [4, 6, 7], which is close to that of WO_3.

The growth of NiO films has been investigated using various techniques such as chemical vapor deposition [18, 19], spin coating [20, 21], sol-gel method [22, 23], pulsed laser deposition [9, 24], spray pyrolysis [25, 26], and radio frequency/direct current sputtering [14, 27–30]. Radio frequency sputtering is a convenient technique because

*Corresponding author
Email address: sanmaikel23@gmail.com (Juan R. Abenuz Acuña)

offers a better control over the deposition parameters such as thickness, substrate temperature, and transfer of the exact chemical composition [31]. Previous work has focused on investigating how electrochromic properties are affected by deposition parameters as annealing temperature, oxygen concentration, substrate temperature, etc. [2, 3, 7–9]. However, to our knowledge there are no works assessing the effect of sputtering power on the electrochromic properties.

In this research we investigate the sputtering power effects on the electrochromic properties of NiO films grown by radio frecuency (RF) magnetron sputtering. Crystalline properties and morphology were characterized using X-ray diffraction (XRD) and scanning electron microscopy (SEM) respectively. Electrochromic properties were evaluated with cyclic voltammetry and chronoamperometry using a solution of lithium perchlorate in propylene carbonate ($LiClO_4-PC$). In order to study the chemical composition before and after Li intercalation X-ray photoelectron spectroscopy (XPS) measurements were performed. The present work is valuable to establish the sputtering power as a parameter for manipulating the electrochromic properties of NiO-based ECD.

2. Experimental

2.1. Film growth and annealing

Two groups conformed by three nickel oxide films with a thickness of 200 nm were deposited using a RF magnetron sputtering system Kurt J. Lesker with a 300 W power supply. One set of films were grown on ITO/glass substrates using a nickel target (99.99% purity) at different sputtering power, that is: P=(60, 140, 180) W and so were labeled S60, S140, and S180, respectively. ITO/glass substrates were acquired from MTI corporation with an area of 3 cm × 1 cm. The thickness of the glass layer is 2.2 mm and that one of ITO is about 200 nm. The other set of films were grown on Si(100) substrates at the same sputtering powers. To obtain the NiO phase, the two groups of films were exposed to a postdeposition heat treatment inside the vacuum chamber for 1 hour at 200°C under an oxygen atmosphere (99.95% purity) at 101×10^3 N/m^2. Table 1 gives a summary of the deposition parameters. The films deposited on Si substrates were just used to check sample crystallinity and the others were used for the rest of the study.

P/W	60, 140, 180
Target	Ni (99.99%)
Substrate type	Si(100) and ITO/glass
T_s/°C	25
P_B/(N/m^2)	0.013
P_{Ar}/(N/m^2)	1.3

Table 1: Deposition parameters for the films: sputtering power (P), target type, substrate type, substrate temperature (T_s), base pressure (P_B), Ar partial pressure (P_{Ar}) .

2.2. Characterization

To study the crystalline properties, films were characterized using a diffractometer Siemens model D-5000 with Cu K alpha radiation (λ_0=1.540 Å). XRD patterns were taken at steps of 0.02° with a time per step of 3 s in a Bragg-Brentano configuration, with a voltage of 34 kV and a current of 25 μA. For morphology study we used a scanning electron microscope Hitachi su5000. The images of the films deposited at P=60 W were taken with a magnification of 500 kX and voltage of 15 kV. The films deposited at higher P were measured with a magnification of 100 kX and voltage of 20 kV. We used a different magnification for S60 because we wanted to observe the film texture and compute the number of grain boundaries. The surface of S60 is pretty smooth and diffused and at the same magnification as the others the grain boundaries cannot be visualized (and thus quantified). The transmittance of the samples before Li intercalation was evaluated using a UV-VIS system VWR UV-1600PC in a wavelength (λ) range from 250 nm to 1 000 nm. To verify the effect of sputtering power on electrochromism of our samples, cyclic voltametry (CV) and chronoamperometry (CA) measurements were carried out using a CorrTest CS350 electrochemical station in a typical three electrode arrangement. Films were used as working electrodes, and the set was completed with a platinum counter electrode and an Ag/AgCl reference electrode. A cubic optoelectrochemical cell (125 cm^3) was filled with an electrolyte of $LiClO_4$ in propylene carbonate (1 M). Transmittance was measured at λ_0=637 nm, using a high sensitivity light sensor PASCO (model CI-6604) connected to acquisition data system PASCO (model UI-5000). CV measurements were performed between -3 V and 3 V with initial voltage V_0=3 V and scan rate of 100 mV/s during 30 cycles. CA curves were obtained between -3 V and 3 V (V_0=3 V) and width step equal to 10 s during 10 steps. To assess the chemical composition of the samples, XPS measurements of the Ni 2p and O 1s core-levels were carried out using a Thermo Fisher Scientific K-alpha XPS spectrometer. Spectra were generated by monochromatic K-alpha radiation (1486.6 eV) with 30° of incident angle between the sample and the X-ray beam. Chemical composition was measured before and after Li intercalation. Resulting spectra were analyzed using CasaXPS software (version 2.3.19PR1.0). A line shape (Gaussian 70% - Lorentzian 30%) defined as GL(30) was used for each component and a standard Tougaard background. Ni spectra were deconvoluted using doublets with splitting of 17.3 eV.

3. Results and discussion

3.1. Crystalline Structure

Samples grown on Si substrates exhibit a diffraction pattern with well localized peaks demonstrating the growth of a crystalline phase (see figure 1). The patterns can

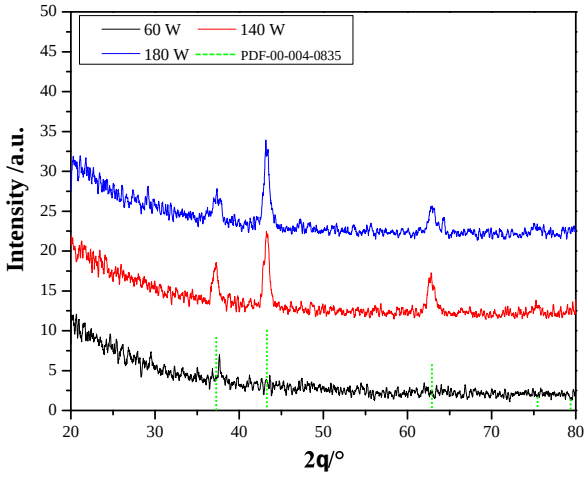

Figure 1: Diffraction pattern for the films deposited at different sputtering powers. Green bars at the bottom correspond to the reference PDF 00-004-0835.

be indexed to the cubic nickel oxide phase (PDF 00-004-0835), with a spatial group $Fm\bar{3}m$, main diffraction peaks at $2\theta = 37°$, $43°$, $62°$, and $75°$; and lattice parameter $a = 4.17$ Å. In the case of S60, diffraction peaks corresponding to the crystallographic planes (111) appear with low intensity, an indicative of a low crystallinity. We believe that this is due to the low energy of most of the Ni atoms ejected from the target. As the low energy atoms arrived at the substrate surface, they do not have enough energy to be trapped and only those with enough energy are captured and reside in lattice sites, favoring an amorphous phase of Ni [32–34].

During the annealing process vacancies are generated and oxygen is adsorbed from the environment tending to form the cubic phase of NiO, however given the amorphous nature of Ni layers, a longer annealing time is required for the atoms to diffuse and order periodically thus manifesting low crystallinity. This is reasonable, for increasing P, most atoms from the target have enough energy to be captured by the substrate and reside in preferential sites, this in turn promotes, during annealing, the crystal ordering around these sites and thus inducing the appearance of diffraction peaks corresponding to crystallographic planes (111), (200), (220), and (311) as can be seen in the rest of the films. All these films showed a preferential orientation along the (200) plane. The crystallite size (D_c) of the samples was estimated for the most intense peak according to Scherrer equation:

$$D_c = \frac{K\lambda_0}{\beta \cos\theta} \qquad (1)$$

where $K = 0.9$, $\lambda_0 = 1.540$ Å, and β is the full width at half maximum of a peak. Results obtained for crystallite size were 119 nm, 11 nm and 15 nm for S60, S140 and S180, respectively.

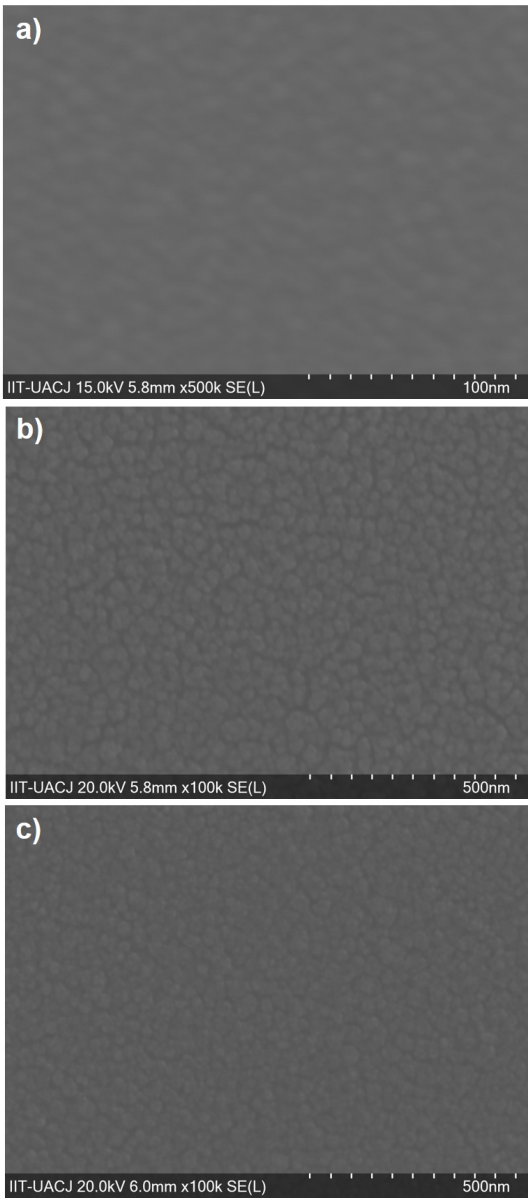

Figure 2: Morphology for films a) S60, b) S140 and c) S180. See text for details.

3.2. Morphology

The morphology of the films is shown in figure 2. The analysis reveals the presence of a smooth granular composition, with diluted roughness for S60. A smooth surface is expected for low sputtering powers since deposition takes place with low energy atoms. In the case of S140 and S180, the morphology is also granular but coarse, with marked grain boundaries. A. Ahmed et al. grew several NiO films at 200 W with RF sputtering technique and reported a morphology similar to ours [35]. The images of figure 2 were used to estimate the average grain size and the percentage of area occupied by the grain boundaries as a function of P (see table 2). By comparison we see that the values show a similar trend, the lowest values for D_G

Sample	D_G/nm	Percentage of area occupied by grain boundaries/ %
S60	10.1±0.1	32±0.6
S140	32.1±0.8	36±0.3
S180	28.7±0.6	33±0.3

Table 2: Average grain size and percentage of area occupied by grain boundaries for all samples.

and the percentage of area are for S60, as a result of increment in sputtering power S140 exhibits the highest values and then decreases for S180. The lowest value in the area occupied by grain boundaries of sample S60 can be therefore related to the regular shape that the grains exhibit and the absence of cracks on the surface. On the other hand, increment in the area occupied by grain boundaries for the others samples can be associated to the morphology showed by the samples S140 and S180 with noticeable cracks on surface [35].

3.3. Electrochromic properties

In order to study the effect of sputtering power on the electrochromic properties of NiO films chronoamperometry (CA), cyclic voltammetry (CV) and transmittance measurements were performed for all samples. Before Li intercalation the effect of P on the transmittance of films was evaluated. Figure 3 shows the transmittance for all samples. Overall, the transmittance decreases as P increases. The higher transmittance measured for S60 can be related to the lowest crystal ordering of this film.

Curves obtained from electrochromic measurements are shown in figure 4. CA and transmittance for S60, S140 and S180 (figure 4a, c and e respectively) show that coloring process shows up during negative current density and

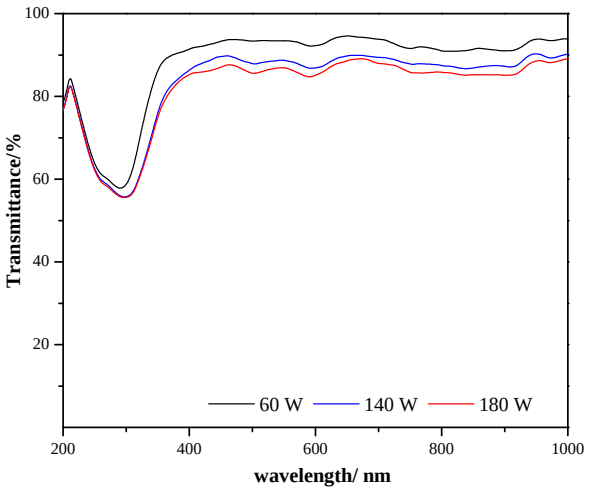

Figure 3: Trasmittance for a) S60, b) S140 and c) S180 before Li intercalation.

the bleached process for positive current density [4]. Coloration efficiency (CE) is the most important property for electrochromic materials and it is defined as

$$CE = \left| \frac{\Delta OD}{\Delta Q} \right| \tag{2}$$

where

$$\Delta OD = \ln\left(\frac{T_b(\lambda_0)}{T_c(\lambda_0)}\right) \tag{3}$$

is called the optical density and ΔQ the inserted or extracted charge. T_b and T_c are the transmittance in bleached and colored states at wavelength λ_0.

Coloration efficiencies are 8.02 cm^2/A·s, 4.81 cm^2/A·s and 3.52 cm^2/A·s for S60, S140, and S180, respectively (table 3). This indicates that sputtering power affects the electrochromic properties, reducing the CE as P increases. As we have found above, such changes can be attributed to variations in cristallinity and morphology (figures 1 and 2). According to Kailing Zhou et al. amorphous NiO films with a further improvement in cristallinity exhibits higher values of CE as a result of large amounts of active sites for electrolyte diffusion. Consequently an enhancement in crystal ordering generates the decrement of CE [5] as occurs here. Possibly the improvement in crystallinity with P intensifies the variations in lattice stress and rises the formation of defects as a consequence of Li insertion/extraction that reduces the absorption and transmission of light. Complementary, the increase in average grain size and area occupied by grain boundaries as P increases (figures 2 and table 2) contributes to high stress and a large expansion/contraction of grains due to Li intercalation that provokes the mechanical deterioration of the film [5, 7] affecting the change in transmittance and CE.

CV measurements for all samples are shown in figures 4b, d and f respectively, only cycles 10, 20 and 30 were plotted. Inset figures display the transmittance for all cycles. In the loops for S60 and S140 (figure 4b and d) we observe that the current density at oxidation peak remains stable around 1.18 mA/cm^2 at -0.38 V and 2.06 mA/cm^2 at -0.46 V respectively. The graph for S180 (figure 4f) exhibits an increment from 1.62 mA/cm^2 to 1.94 mA/cm^2 as the number of cycles rises, suggesting a high reaction activity [36]. Reduction peak was analyzed and S60 shows the peak around 0.043 mA/cm^2 at -0.98 V just for cycle 10. The increase in current density beyond the reduction peak for all samples is probably related to a high electron conductivity

Sample	$\frac{\Delta T}{\%}$	ΔOD	$\frac{\Delta Q}{(\mathbf{A}\cdot\mathbf{s})\cdot\mathbf{cm}^{-2}}$	$\frac{CE}{\mathbf{cm}^2\cdot(\mathbf{A}\cdot\mathbf{s})^{-1}}$
S60	60.3	0.99	-0.12	8.02
S140	51.4	0.92	-0.19	4.81
S180	35.7	0.64	-0.18	3.52

Table 3: Electrocromic properties for the samples: Optical modulation (ΔT), change in optical density (ΔOD), charge difference (ΔQ) and coloration efficiency (CE).

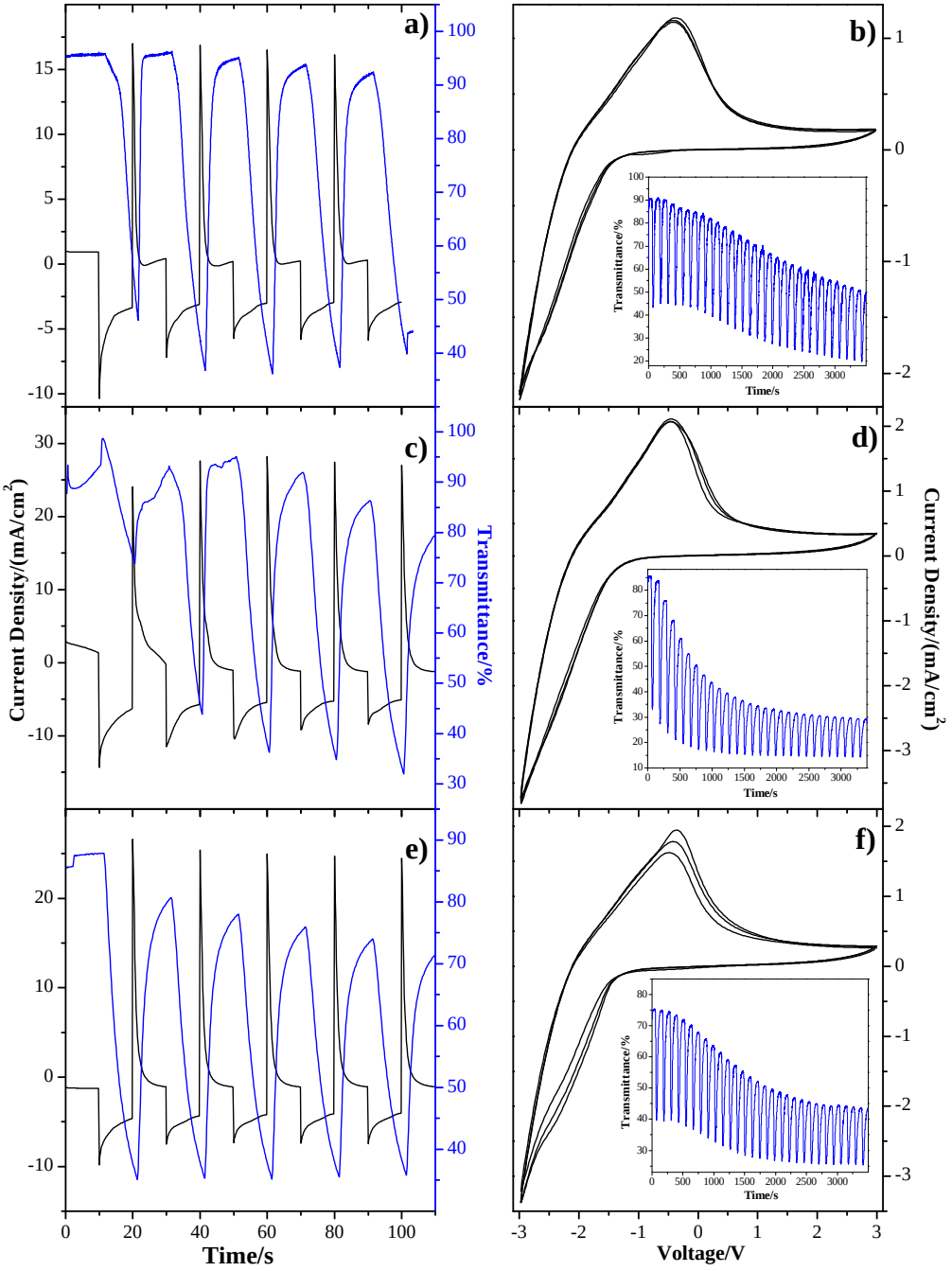

Figure 4: Chronoamperometry and transmittance for S60 (a), S140 (c), and S180 (e); and cyclic voltammetry and transmittance (insets) for S60 (b), S140 (d), and S180 (f).

in the colored state and internal electronic leakage arising from defects such as metallic particles, pinholes and dust, as a consequence the current density is composed of kinetic transfer of Li^+ ions, reversely kinetic transfer of the charge-balancing electrons and leakage-inducing electrons [4]. Cycles 20 and 30 reveal the absence of the reduction peak suggesting a higher contribution from leakage current. S140 does not exhibit a reduction peak in any cycle while S180 and S60 exhibit a similar behavior in the 10 cycle with a current density peak at -0.77 V. The transmittance and therefore the optical modulation decreases as the number of cycles evolve.

The maximum transmittance dependence of the sputtering power after the first cycle was analyzed for the three

Figure 5: (Color online) S60 dipped in the electrolite solution in the bleached (left) and colored (right) states at a bias of −3 V

samples. We observe a decrement of the transmittance from 90.8% at 60 W to 75% at 180 W; indicating that higher sputtering powers reduced the maximum transmittance. Since we have determined that higher sputtering power favors the crystallinity of films, larger grain boundaries and larger grains, this seems to affect also the Li intercalation, the absorption of light and thus the transmittance. Electrochromic measurements suggest that electrochromic properties of NiO changes by varying the sputtering power P.

3.4. Chemical analysis

XPS measurements were performed for all samples before and after Li intercalation to study the effect of sputtering power on the chemical composition. Li intercalation was attained by dipping the sample in the electrolite and

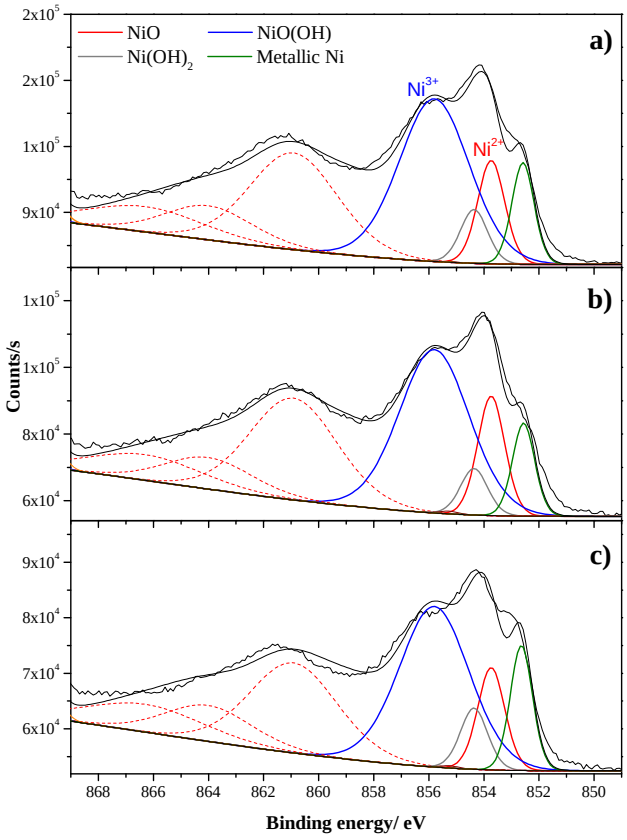

Figure 6: XPS spectra for Ni $2p_{3/2}$ core-level of a) S60, b) S140 and c) S180 before Li intercalation.

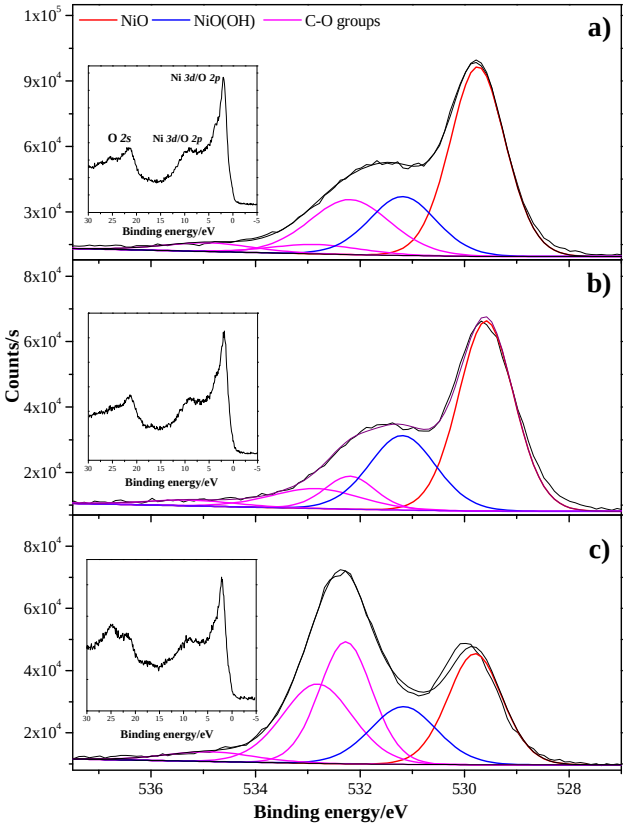

Figure 7: XPS spectra for O 1s core-level of a) S60, b) S140 and c) S180 before the Li intercalation. Inset show the core-levels near to Fermi level.

applying a bias of −3 V for 1 s, thus leaving the samples in the colored state (see figure 5). The spectra for Ni $2p_{3/2}$ and O $1s$ core-levels of S60, S140 and S180 before Li intercalation are presented in the figures 6 and 7, respectively. We just show the Ni $2p_{3/2}$ signal since this part of the spectrum contains the most relevant information on the oxidation states of nickel. A peak at 853.7 eV in the Ni spectra is observed, corresponding to Ni^{2+} for NiO phase. Peaks at 854.3 eV and 855.8 eV are attributed to $Ni(OH)_2$ and NiO(OH) (oxidation state Ni^{2+} and Ni^{3+}, respectively) [37–41].

According to Rui-Tao et al. [3], OH^- groups can be adsorbed on the surface of NiO films when there are small amounts of water. The presence of both NiO(OH) and $Ni(OH)_2$ in our samples can be associated to water adsorbed from the environment during film manipulation. These peaks suggest an admixture of these compounds on the surface, however, the $Ni(OH)_2$ signal is lower than the signal of NiO(OH), indicating a higher presence of this last nickel hydroxide [24, 40, 42]. We also analyzed the C $1s$ core-level (not shown) and observed carbon contamination which is adsorbed mainly during film manipulation, suggesting that the water comes also from the environment. One peak at 852.5 eV is observed for all samples that is due to the presence of metallic Ni [40, 41]. Perhaps, its presence is associated to reduction of nickel atoms present in different nickel compounds as a result of the annealing process, especially at the surface [43]. Peaks observed beyond 860 eV (red dash lines) are attributed to shake-up satellites [44].

The O $1s$ core-level are presented in figure 7. A low binding energy peak at 529.7 eV corresponding to NiO phase appears. The peak at 531.2 eV can be attributed to NiO(OH) [37–41]. Peaks observed at higher binding energies (532.2 eV) can be related to organic contamination such as carbon which is ubiquitous in most samples and is adsorbed easily when the samples are exposed to the environment [40]. To confirm the presence of NiO phase, we also measured the valence band (insets in figure 7). The typical spectra corresponding to NiO is observed for all samples, with peaks at (1.9, 8.9) eV associated to hybridization of Ni $3d$ and O $2p$ core-levels (Ni $3d$/O $2p$). Another peak appears at 21.3 eV corresponding to O $2s$ core-level. These results suggest a high presence of NiO and a hydroxilation of the surface. To determine the oxygen and nickel concentration for NiO phase in our samples, we computed the oxygen to nickel ratio (O/Ni) by estimating the area under the peaks of Ni $2p$ and O $1s$ core-levels, respectively. The ratios were 1.33, 1.15, and 1.39 for S60,

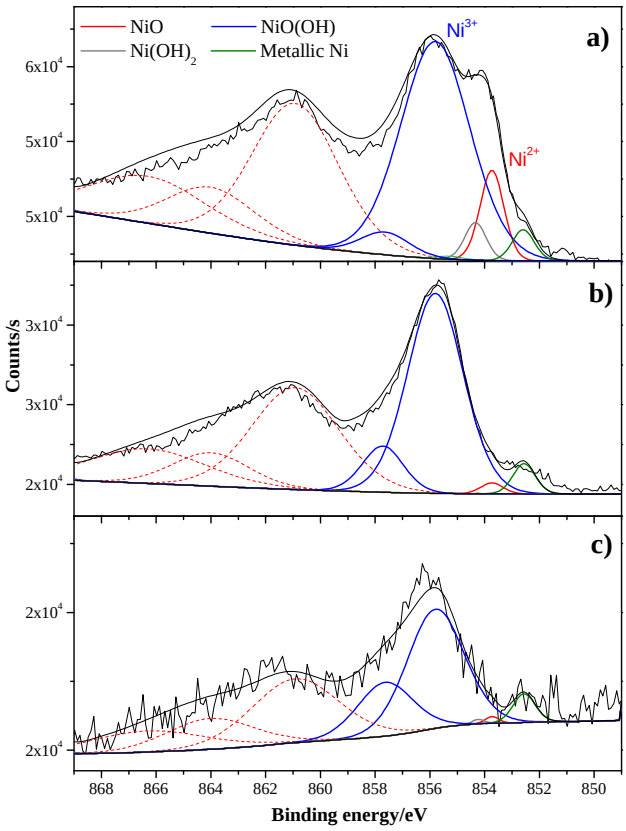

Figure 8: XPS spectra for Ni $2p_{3/2}$ core-level of a) S60, b) S140 and c) S180 after the Li intercalation.

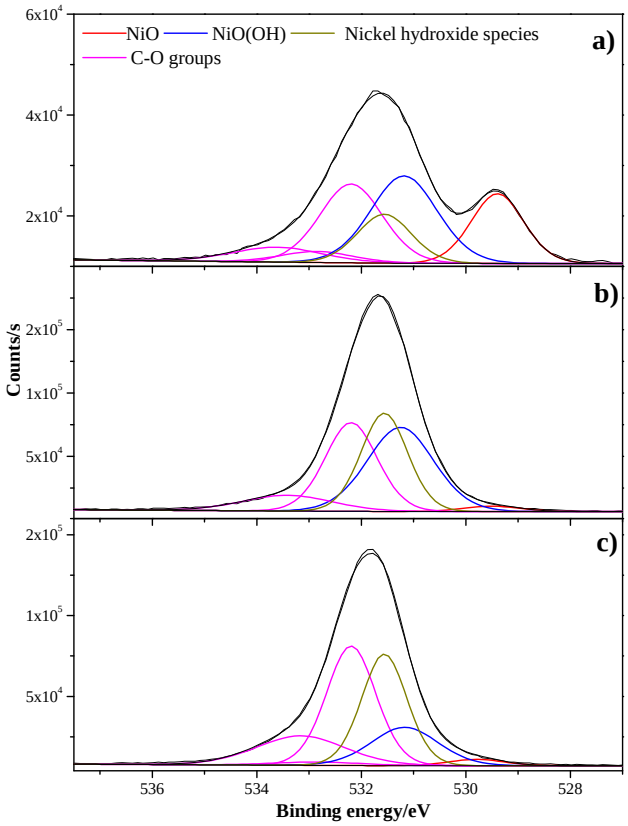

Figure 9: XPS spectra for O $1s$ core-level of a) S60, b) S140 and c) S180 after the Li intercalation.

S140 and S180, respectively. Accordingly, these results imply the formation of nickel hydroxides at the surface and the nonstoichiometry of the samples, suggesting that sputtering power affects the oxygen and nickel concentration. Previous studies have reported an O/Ni ratio between 1.5 and 2 for both NiO(OH) and $Ni(OH)_2$ [39].

To study the effect of P on the chemical composition and their relationship with changes in electrochromic properties XPS spectra were analyzed after Li intercalation. The spectra for Ni $2p_{3/2}$ and O $1s$ core-levels for all samples in the colored state are shown in figures 8 and 9 respectively. For the Ni $2p_{3/2}$ core-level we identify the same peaks as in the previous case. In addition to these peaks, another signal is spotted at 857.6 eV that can be associated to nickel hydroxides species [39–41], possibly NiO(OH) or $Ni(OH)_2$. We observe that the Ni^{2+} signal diminishes as P increases while the signal attributed to nickel hydroxide species increases. The spectra of the O $1s$ core-level (figure 9) show the same behavior as in the previous case, however a new peak at 531.5 eV, related to nickel hydroxides [39–41, 45], appears for all samples. It is evident that the signal associated to NiO (Ni^{2+}) decreases as P increases while the signal related to nickel hydroxides at 531.5 eV increases. We thus assume that hydroxylation of surface is taking place at higher sputtering powers. Our findings strongly indicate that, after interacting with OH^- ions, NiO reversibly turns into NiO(OH) and from $NiO(OH)_2$ to NiO(OH) [3, 24]. The existence of these nickel species on the film surface before Li intercalation (figure 6 and 7) in addition to the presence of OH^- groups in the electrolyte as a result of small amounts of water, apparently contributes to chemical mechanisms that facilitate the appearance of nickel hydroxides. Moreover, as a result of changes in the morphology and crystallinity with changes in P, large quantities of Li ions may be inserted and extracted from the film, rising the number of chemical reactions that promote the hydroxilation of the film.

According to the preceding discussion, one realizes that before Li intercalation, XPS analysis reveals the presence of both NiO and nickel hydroxides on the surface. Also we observe an effect of the sputtering power on the stoichiometry of NiO. After Li intercalation, we observe the same oxidation states as in the previous case, however the atomic concentration of the Ni hydroxides largely differs from that before Li intercalation. Therefore, it is clear that changes in crystallinity and morphology driven by variations in sputtering power have an impact on the formation of Ni hydroxides.

4. Conclusions

We deposited nickel oxide films at different sputtering powers (60 W-180 W). Both film crystallinity and morphology were affected by the changes in sputtering power. The XRD characterization showed diffraction patterns corresponding to cubic NiO, manifesting a change in the preferential orientation of the films, from the (111) crystallographic plane to the (200) plane as P increases. We found a close relationship between the average grain size and the area occupied by grain boundaries as a function of P. Both quantities follow a similar tendency. S60 shows the highest value of CE and drops for the other samples; this behavior is related to the reduction of optical density as P increases. For CV measurements the maximum transmittance in bleached states after the first cycle also reduces as P increases. CA and CV measurements indicate that as P increases CE diminishes. Chemical composition determined with XPS technique before Li intercalation shows the presence of several phases such as NiO, NiO(OH), $Ni(OH)_2$ and metallic Ni. The valence band as well as the O/Ni ratio for all samples suggest that films are mainly composed of NiO and the partial hydroxilation of surface. After Li intercalation chemical composition exhibit a relationship with P indicating that hydroxylation of the surface is promoted at higher sputtering power as a result of a possible increase in Li insertion in the film lattice stimulated by the different morphologies and crystallinities of the samples.

Results obtained from this research invariably indicate that crystalline properties, morphology, chemical composition and electrochromic properties of NiO films deposited by RF sputtering can be altered trough sputtering power variations.

Acknowledgements

We are grateful to Dra. Claudia Rodríguez, Daniel Aguilar, William Cauich, and Hortensia Reyes for their technical support in the XRD, SEM, and XPS sessions. The authors gratefully acknowledge the support from the National Council of Science and Technology through grant INFR-2019-301724 for SEM maintenance, the program Cátedras CONACYT project 3035, and partial support from the Universidad Autónoma de Ciudad Juárez through project PIVA 334-18-12.

References

[1] G. Atak and D. Cokun, Annealing effects of NiO thin films for all-solid-state electrochromic devices, Solid State Ionics 305,(2017)43-51 .

[2] H. Moulki, C. Faure, M. Mihelcic, A. Surca Vuk, F. Svegl, B. Orel, G. Campet, M. Alfredsson, A.V. Chadwick, D. Gianolio, A. Rougier, Electrochromic performances of nonstoichiometric NiO thin fi lms, Thin Solid Films 553, (2014) pp. 63–66.

[3] R. Wen, C.G. Granqvist, and G.A. Niklasson, Anodic Electrochromism for Energy-Effi cient Windows : Cation / Anion-Based Surface Processes and Effects of Crystal Facets in Nickel Oxide Thin Films, Advanced Functional Materials, (2015) pp. 3359–3370.

[4] Q. Liu, G. Dong, Q. Chen, J. Guo, Y. Xiao, Solar Energy Materials and Solar Cells Charge-transfer kinetics and cyclic properties of inorganic all-solid-state electrochromic device with remarkably improved optical memory, Solar Energy Materials and Solar Cells 174, (2018) pp. 545–553.

[5] K. Zhou, Z. Qi, B. Zhao, S. Lu, H. Wang, J. Liu, H. Yan, The influence of crystallinity on the electrochromic properties and

durability of NiO thin films, Surfaces and Interfaces 6, (2017) pp. 91–97.
[6] P. Yang, P. Sun, and W. Mai, Electrochromic energy storage devices, Materials Today 19, (2016) pp. 394–402.
[7] Q. Liu, G. Dong, Y. Xiao, M. Delplancke-ogletree, Electrolytes-relevant cyclic durability of nickel oxide thin films as an ion-storage layer in an all-solid-state complementary electrochromic device, Solar Energy Materials and Solar Cells 157, (2016) pp. 844–852.
[8] X. Song, G. Dong, F. Gao, Y. Xiao, Q. Liu, Properties of NiO_x and its in fluence upon all-thin-film ITO/NiO_x/ $LiTaO_3$/WO_3/ITO electrochromic devices prepared by magnetron sputtering, Vacuum 111, (2015) pp. 48–54.
[9] Y. He, T. Li, X. Zhong, M. Zhou, G. Dong, X. Diao, Lattice and electronic structure variations in critical lithium doped nickel oxide thin film for superior anode electrochromism, Electrochimica Acta 316, (2019) pp. 143–151.
[10] A. Mahmoudi, H. I. Faraoun, M.K. Benabadji, I. Abdellaoui, M. Dergal, Structural, electronic and optical properties of Li intercalated on MO_3 (M: Mo, W): A first principle investigation," Solid State Communications 229, (2016) pp. 37–42.
[11] R.T. Wen, C.G. Granqvist, G.A. Niklasson, Eliminating degradation and uncovering ion-trapping dynamics in electrochromic WO_3 thin films, Nature Materials 14, (2015) pp. 996–1001.
[12] M.V. Limaye, J.S. Chen, S.B. Singh, Y.C. Shao, et al., Correlation between electrochromism and electronic structures of tungsten oxide films, Royal Society of Chemistry 4, (2014) pp. 5036–5045.
[13] R.C. Korošec and P. Bukovec, Sol-Gel Prepared NiO Thin Films for Electrochromic Applications, Acta Chimica Slovenica 53, (2006) pp. 136–147.
[14] H.L. Chen, Y.M. Lu, W. S. Hwang, Characterization of sputtered NiO thin films, Surface and Coatings Technology 198, (2005) pp. 138-142.
[15] R. Kumar, C. Baratto, G. Faglia, G. Sberveglieri, E. Bontempi, L. Borgese, Tailoring the textured surface of porous nanostructured NiO thin films for the detection of pollutant gases, Thin Solid Films 583, (2015) 233-238.
[16] I. Hotovy, J. Huran, L. Spiess, Characterization of sputtered NiO films using XRD and AFM. Journal of Materials Science 39, (2004) 2609-2612.
[17] S.Y. Park, H.R. Kim, Y.J. Kang, D.H. Kim, J.W. Kang, Organic solar cells employing magnetron sputtered p-type nickel oxide thin film as the anode buffer layer, Solar Energy Materials and Solar Cells 94, (2010) 2332-2336.
[18] M.A. Vidales-Hurtado and A. Mendoza-Galván, Electrochromism in nickel oxide-based thin films obtained by chemical bath deposition, Solid State Ionics 179, (2008) pp. 2065–2068.
[19] X.H. Xia, J.P. Tu, J. Zhang, X.L. Wang, W.K. Zhang H. Huang, Electrochromic properties of porous NiO thin films prepared by a chemical bath deposition, Solar Energy Materials and Solar Cells 92, (2008) pp. 628–633.
[20] I. Sta, M. Jlassi, M. Hajji, H. Ezzaouia, Structural, optical and electrical properties of undoped and Li-doped NiO thin films prepared by sol–gel spin coating method, Thin Solid Films 555, (2014) pp. 131–137.
[21] A.A. Al-Ghamdi, W.E. Mahmoud, S.J. Yaghmour, F.M. Al-Marzouki, Structure and optical properties of nanocrystalline NiO thin film synthesized by sol–gel spin-coating method, Journal of Alloys and Compounds 486, (2009) pp. 9–13.
[22] A.M. Soleimanpour, Y. Hou, A.H. Jayatissa, Evolution of hydrogen gas sensing properties of sol–gel derived nickel oxide thin film, Sensors Actuators B. Chemical 182, (2013) pp. 125–133.
[23] A.M. Soleimanpour and A.H. Jayatissa, Preparation of nanocrystalline nickel oxide thin films by sol–gel process for hydrogen sensor applications, Materials Science and Engineering: C 32, (2012) pp. 2230–2234.
[24] Y. Abe, T. Suzuki, M. Kawamura, K. Sasaki, H. Itoh, Electrochromic properties of NiOOH thin films prepared by reactive sputtering in an H_2O atmosphere in various aqueous electrolytes, Solar Energy Materials and Solar Cells 99, (2012) pp. 38–42.
[25] K.H. Abass, Spray Pyrolysis Deposition and Effect of Annealing Temperature on Optical Properties of Cu:NiO Film, International Letters of Chemistry, Physics and Astronomy 47, (2015) pp. 178–184.
[26] R.A. Ismail, S. Ghafori, G.A. Kadhim, Preparation and characterization of nanostructured nickel oxide thin films by spray pyrolysis, Applied Nanoscience 3, (2013) pp. 509–514.
[27] M. Guziewicz et al., Hydrogen Sensing Properties of Thin NiO Films Deposited by RF Sputtering, Procedia Engineering 47, (2012) pp. 746–749.
[28] A.M. Reddy, A.S. Reddy, K.S. Lee, P.S. Reddy, Growth and characterization of NiO thin films prepared by dc reactive magnetron sputtering, Solid State Science 13, (2011) pp. 314–320.
[29] J. Keraudy, J. García, A. Ferrec, B. Corraze, M. Richard-Plouet, A. Goullet, P.Y Jouan, Structural, morphological and electrical properties of nickel oxide thin films deposited by reactive sputtering, Applied Surface Science 357, (2015) pp. 838–844.
[30] M. Guziewicz, W. Jung, J. Grochowski, M. Borysiewicz, K. Golaszewska, R. Kruszka, et al., Influence of thermal and gamma radiation on electrical properties of thin NiO films formed by RF sputtering, Procedia Engineering 25, (2011) pp. 367–370.
[31] A.A. Al-Ghamdi, M.S. Abdel-wahab, A.A. Farghali, P.M.Z. Hasan, Structural, optical and photo-catalytic activity of nanocrystalline NiO thin films. Materials Research Bulletin 75, (2016) pp. 71-77.
[32] J.A. Thornton, Influence of apparatus geometry and deposition conditions on the structure and topography of thick sputtered coatings, Journal of Vacuum Science and Technology 11, (1974) pp. 666-670.
[33] N Kaiser, Review of the fundamentals of thin-film growth, Applied Optics 41, (2002) pp. 3053-3060.
[34] A. Anders, A structure zone diagram including plasma-based deposition and ion etching, Thin Solid Films 518, (2010) pp. 4087-4090.
[35] A.A. Ahmed, M. Devarajan, N. Afzal, Effects of substrate temperature on the degradation of RF sputtered NiO properties, Materials Science in Semiconductor Processing 63, (2017) pp. 137-141.
[36] X.H. Xia, J.P. Tu, J. Zhang, X.L. Wang, W.K. Zhang, H. Huang, Electrochromic properties of porous NiO thin films prepared by a chemical bath deposition, Solar Energy Materials and Solar Cells 92, (2008) pp. 628–633.
[37] M. Tyagi, M. Tomar, V. Gupta, Postdeposition annealing of NiO_x thin films: A transition from n-type to p-type conductivity for short wave length optoelectronic devices, Journal of Materials Research 28, (2013) pp. 723-732.
[38] I. Saric, R. Peter, I. Kavre, I.J. Badovinac, M. Petravic, Oxidation of nickel surfaces by low energy ion bombardment, Nuclear Instruments and Methods in Physics Research, Section B: Beam Interactions with Materials and Atoms 371, (2016) pp. 286–289.
[39] B.P. Payne, M.C. Biesinger, N.S. McIntyre, Use of oxygen/nickel ratios in the XPS characterisation of oxide phases on nickel metal and nickel alloy surfaces, Journal of Electron Spectroscopy and Related Phenomena 185, (2012) pp. 159–166.
[40] B.P. Payne, M.C. Biesinger, N.S. McIntyre, The study of polycrystalline nickel metal oxidation by water vapour, J.Journal of Electron Spectroscopy and Related Phenomena 175, (2009) pp. 55–65.
[41] M.C. Biesinger, B.P. Payne, L.W.M. Lau, A. Gerson, R.S.C. Smart, X-ray photoelectron spectroscopic chemical state Quantification of mixed nickel metal, oxide and hydroxide systems,Surface and Interface Analysis 41, (2009) pp. 324–332.
[42] A. Van Der Ven, D. Morgan, Y.S. Meng, G. Ceder, Phase stability of nickel hydroxides and oxyhydroxides, Journal of the Electrochemical Society 153, (2006) pp. 210–215.
[43] S. Oswald and W. Brückner, XPS depth profile analysis of non-stoichiometric NiO films, Surface and Interface Analysis 36, (2004) pp. 17–22.

[44] A.N. Mansour, Characterization of NiO by XPS, Surface Science Spectra 3, (1994) pp. 231–238.
[45] A.F. Carley and S. Rassias, The Specificity of Surface Oxygen in the Activation, Surface Science 135, (1983) pp. 35–51.

Highlights

- Nickel oxide films were grown on ITO-glass at different sputtering power (*P*).
- We study the effects of *P* on the electrochromic properties of the samples.
- We found that *P* affects the crystalline structure and morphology.
- The hydroxylation of the surface is promoted at higher *P*.
- Coloration efficiency reduces as *P* increases.

Declaration of interests

☒ The authors declare that they have no known competing financial interests or personal relationships that could have appeared to influence the work reported in this paper.

☐The authors declare the following financial interests/personal relationships which may be considered as potential competing interests: